NeuroImage: Clinical 37 (2023) 103307

Contents lists available at ScienceDirect

NeuroImage: Clinical

journal homepage: www.elsevier.com/locate/ynicl

Neural correlates of impulsive compulsive behaviors in Parkinson's disease: A Japanese retrospective study

Ikko Kimura [a,b], Gajanan S. Revankar [a], Kotaro Ogawa [a], Kaoru Amano [b,c], Yuta Kajiyama [a,*,1], Hideki Mochizuki [a,*,1]

[a] Department of Neurology, Osaka University Graduate School of Medicine, Suita 565-0871, Japan
[b] Graduate School of Frontier Biosciences, Osaka University, Suita 565-0871, Japan
[c] Graduate School of Information Science and Technology, The University of Tokyo, Tokyo 113-8656, Japan

ARTICLE INFO

Keywords:
Parkinson's disease
Impulsive compulsive behaviors
Functional connectivity
Voxel-based morphometry
Cortico-striatal network

ABSTRACT

Background: Impulsive compulsive behaviors (ICBs) often disturb patients with Parkinson's Disease (PD), of which impulse control disorder (ICD) and dopamine dysregulation syndrome (DDS) are two major subsets. The nucleus accumbens (NAcc) is involved in ICB; however, it remains unclear how the NAcc affects cortical function and defines the different behavioral characteristics of ICD and DDS.

Objectives: To identify the cortico-striatal network primarily involved in ICB and the differences in these networks between patients with ICD and DDS using structural and resting-state functional magnetic resonance imaging.

Methods: Patients with PD were recruited using data from a previous cohort study and divided into those with ICB (ICB group) and without ICB (non-ICB group) using the Japanese version of the Questionnaire for Impulsive Compulsive Disorders in Parkinson's Disease (J-QUIP). From these two groups, we extracted 37 pairs matched for age, sex, disease duration, and levodopa equivalent daily dose of dopamine agonists. Patients with ICB were further classified as having ICD or DDS based on the J-QUIP subscore. General linear models were used to compare gray matter volume and functional connectivity (FC) of the NAcc, caudate, and putamen between the ICB and non-ICB groups and between patients with ICD and those with DDS.

Results: We found no significant differences in gray matter volume between the ICB and non-ICB groups or between patients with ICD and those with DDS. Compared with the non-ICB group, the FC of the right NAcc in the ICB group was lower in the bilateral ventromedial prefrontal cortex and higher in the left middle occipital gyrus. Furthermore, patients with DDS showed higher FC between the right putamen and left superior temporal gyrus and higher FC between the left caudate and bilateral middle occipital gyrus than patients with ICD. In contrast, patients with ICD exhibited higher FC between the left NAcc and the right posterior cingulate cortex than patients with DDS.

Conclusions: The functionally altered network between the right NAcc and ventromedial prefrontal cortex was associated with ICB in PD. In addition, the surrounding cortico-striatal networks may differentiate the behavioral characteristics of patients with ICD and those with DDS.

1. Introduction

Parkinson's disease (PD) is a neurodegenerative disease characterized by the deposition of alpha-synuclein and the degeneration of dopamine-producing cells in the substantia nigra (Rocha et al., 2018). Patients with PD present various motor and non-motor symptoms, including impulsive compulsive behaviors (ICBs). ICB is a state where patients are unable to resist a certain urge or impulse, and 6–34.8 % of

Abbreviations: PD, Parkinson's disease; ICB, impulsive compulsive behaviors; ICD, impulse control disorder; DDS, dopamine dysregulation syndrome; FC, functional connectivity; GMV, gray matter volume; NAcc, nucleus accumbens; J-QUIP, Japanese version of the Questionnaire for Impulsive Compulsive Disorders in Parkinson's Disease; DRT, dopamine replacement therapy; DA, dopamine agonists; rsfMRI, resting-state functional magnetic resonance imaging; LEDD, levodopa equivalent daily dose; CSF, cerebrospinal fluid; WM, white matter; GM, gray matter; FWHM, full-width half maximum; FD, framewise displacement; TBV, total brain volume; vmPFC, ventromedial prefrontal cortex; MOG, middle occipital gyrus; STG, superior temporal gyrus; PCC, posterior cingulate cortex.

* Corresponding authors at: 2-2, Yamada-oka, Suita 565-0871, Japan.
E-mail addresses: kajiyama@neurol.med.osaka-u.ac.jp (Y. Kajiyama), hizuki@neurol.med.osaka-u.ac.jp (H. Mochizuki).

[1] These two authors equally contributed to this work.

https://doi.org/10.1016/j.nicl.2022.103307
Received 20 September 2022; Received in revised form 25 December 2022; Accepted 26 December 2022
Available online 28 December 2022

patients with PD suffer from ICB during the treatment course of dopamine replacement therapy (DRT) (Zhang et al., 2014). While DRT improves motor symptoms, it can exacerbate ICB, and no established treatments are available for ICB (Weintraub and Claassen, 2017). Although symptoms associated with ICB worsen patients' quality of life and burden on caregivers (Voon et al., 2017; Weintraub and Nirenberg, 2013), ICB is commonly overlooked in clinical practice as patients hesitate to spontaneously report these behaviors owing to the stigma or denial of their symptoms (Evans et al., 2009; Perez-Lloret et al., 2012). Therefore, objective biomarkers, such as functional connectivity (FC) or gray matter volume (GMV), are required to detect ICB before these symptoms interfere with patients' social lives (Kanai and Rees, 2011; Koike et al., 2021).

The cause of ICB has been attributed to non-physiological dopaminergic stimulation in relatively intact regions of the degenerated cortico-striatal networks in PD, including the nucleus accumbens (NAcc) (Vriend, 2018).

Alpha-synuclein deposition in the NAcc is lower in PD patients with ICB (Barbosa et al., 2019). Moreover, a recent *meta*-analysis of functional imaging studies revealed that the hyperactivation of the NAcc was significantly associated with ICB (Santangelo et al., 2019). However, no consistent results have been reported regarding which alterations in cortico-striatal networks, including the NAcc, cause ICB. While previous studies have revealed alterations in the FC of fronto-striatal networks in the NAcc of patients with ICB (Mata-Marín et al., 2021; Navalpotro-Gomez et al., 2020; Tessitore et al., 2017), others have suggested the involvement of the FC in other subcortical regions, such as the caudate (Gu et al., 2022; Ruitenberg et al., 2018) and putamen (Carriere et al., 2015; Ruitenberg et al., 2018). Previous studies have also shown inconsistent results regarding which regions of the GMV are altered in patients with ICB (Santangelo et al., 2019). One major reason for these inconsistencies is the relatively small sample sizes in each study (Marek et al., 2022).

Another reason for the inconsistent results on the neural correlates of ICB across studies is the heterogeneity of ICB (Weintraub and Claassen, 2017). ICB comprises two major subsets, namely impulse control disorder (ICD; intolerance of resisting an impulse to perform a certain behavior) and dopamine dysregulation syndrome (DDS; compulsive and excessive use of dopaminergic drugs) (Weintraub et al., 2015). Several studies have suggested that levodopa and apomorphine may trigger DDS onset (Lawrence et al., 2003), while other dopamine agonists (DAs) tend to cause ICD (Weintraub et al., 2006), suggesting that different brain regions or mechanisms may be involved in the two symptomologies. Although the reasons for these tendencies are not clear, one possible explanation is the difference in the duration of effect between these drugs, with the effective duration of levodopa or apomorphine being shorter than that of other DAs (Gatto and Aldinio, 2019). This means that levodopa and apomorphine are more likely to induce an unpleasant "off" state than DAs, hence, patients are more likely to crave more drugs to reverse that state to the "on" state (Lawrence et al., 2003). Another possible explanation for the different tendencies between levodopa or apomorphine and other DAs might be the differences in affinity for different types of dopamine receptors (Zhang et al., 2014). Retrospective studies suggest that DA with a high affinity for D_3 receptors, such as pramipexole or ropinirole, are more likely to induce ICD than other drugs (Dodd et al., 2005; Garcia-Ruiz et al., 2014). However, it remains unclear which regions are specifically involved in ICD and DDS development. Hence, identifying the region specific to each ICB subset is essential for identifying novel targets for neuromodulation therapies.

Therefore, this study aimed to identify the cortico-striatal networks most actively involved in the occurrence of ICB, and the differences in these networks between patients with ICD and those with DDS. For this purpose, we conducted a retrospective study to compare the FC of cortico-striatal networks or GMV between patients with and without ICB and between patients with ICD and DDS. We hypothesized that regions associated with the NAcc are functionally or structurally altered in patients with ICB.

2. Material and methods

2.1. Participants

This study was conducted as part of a prospective and exploratory study of disease-specific biomarkers and objective indicators of neurodegenerative diseases at Osaka University (UMIN ID: UMIN000036570), which registered all patients with PD admitted to Osaka University Hospital (Kajiyama et al., 2021; Nakano et al., 2021; Otomune et al., 2019). We obtained data on those with or without ICB. We enrolled patients who met the following inclusion criteria: (1) aged 40–85 years, (2) diagnosed with clinically established or probable PD according to the Movement Disorder Society Parkinson Disease Diagnostic Criteria (Postuma et al., 2015), (3) completed resting-state functional magnetic resonance imaging (rsfMRI) and structural MRI scans, and (4) completed the Japanese version of the Questionnaire for Impulsive-Compulsive Disorders in Parkinson's Disease (J-QUIP). The exclusion criteria were as follows: (1) a history of other neurological or psychiatric diseases and (2) significant neurological abnormalities on MRI scans (e.g., brain tumor or cerebral infarction) evaluated by two neurologists (K.I. and K. Y.). Based on these criteria, 184 patients were included in this study.

2.2. Ethics

This study was approved by the Osaka University clinical research review committee (Approval number: 13471–12) and was performed in accordance with the Declaration of Helsinki. Written informed consent was obtained from all participants.

2.3. Evaluation for ICB

We divided the eligible patients into two groups, namely ICB and non-ICB groups. The ICB group was defined as having a score greater than zero in J-QUIP, whereas the non-ICB group had a score equal to zero (Takeshige-Amano et al., 2022; Tanaka et al., 2013). To investigate the characteristics of ICD and DDS, we further defined patients with ICD as those who responded yes to any item in the following sections of the J-QUIP: A (pathological gambling), B (hypersexuality), C (compulsive buying), and D (binge eating). In contrast, we defined patients with DDS as those who responded yes to any item in section F (DDS) of the J-QUIP.

2.4. Clinical evaluations

The following information was obtained from the registered data to acquire the basic characteristics of each group: age, sex, handedness, dominant side of motor symptoms, disease duration, medications, levodopa equivalent daily dose (LEDD), Apathy Scale, Epworth Sleepiness Scale, Frontal Assessment Battery, Geriatric Depression Scale, Hamilton Depression Rating Scale, Mini-Mental State Examination, Parkinson's Disease Questionnaire-39, and Movement Disorder Society-Sponsored Revision of the Unified Parkinson's Disease Rating Scale scores. Neurological examination and clinical interview by a neurologist were used to determine the dominant side of motor symptoms. The LEDD was calculated according to a previous report (Tomlinson et al., 2010).

2.5. Image acquisition

MRI data were collected using a GE 3-T scanner (GE Medical Systems, WI, USA) in a dark room at Osaka University Hospital. Standard foam pads were placed in the scanner to stabilize patients' heads. rsfMRI data were acquired with axial gradient-echo echo-planar imaging (voxel

size = 3.3×3.3×3.2 mm, slice gap = 0.8 mm, matrix size = 64×64×40, TE = 30 ms, TR = 2.5 s, flip angle = 80°, 240 volumes). During the rsfMRI scans, patients were instructed to keep their eyes fixed on a black cross located at the center of the screen and keep their bodies as steady as possible, without any thoughts in their minds. Structural MRI data were obtained with a T1-weighted sagittal inversion-recovery spoiled-gradient-echo sequence (voxel size = 1.2×1×1 mm, matrix size = 200×256×256, TE = 3.2 ms, TR = 8.2 ms, inversion time = 400 ms). Both MRI scans were performed during the "on" state of each patient.

2.6. Quality control for MRI scans

To ensure the image quality of MRI scans, the data were excluded based on the following criteria: (1) significant motion observed by the visual inspection of structural MRI and rsfMRI data (n = 6) and (2) excessive head motion detected in rsfMRI scans defined as mean framewise displacement (FD) >0.2 mm, exceeded 20 % prevalence of scans with FD >0.5 mm, or maximum FD >5 mm (Parkes et al., 2018) (n = 28). We excluded 34 patients, and the data of the remaining 150 patients were used for further analysis (Fig. 1).

2.7. Image analysis

To conduct FC analysis, T1-weighted and rsfMRI data were preprocessed with the default pipeline of fMRIPrep 20.2.1 (Esteban et al., 2019). T1-weighted data were intensity-normalized, skull-stripped, and tissue-segmented into the cerebrospinal fluid (CSF), white matter (WM), and gray matter (GM). These data were then spatially normalized to the Montreal Neurological Institute nonlinear 6th-generation space (MNI standard space). For the rsfMRI data, we first skull-stripped the entire dataset, defining the first rsfMRI data as the reference for the co-registration to T1-weighted data. The fMRI data were then corrected for motion and slice timing, warped to the MNI standard space, spatially smoothed with a Gaussian kernel of 6 mm full-width half maximum (FWHM), and temporally band-pass filtered between 0.001 and 0.01 Hz. Several nuisance signals were extracted from the preprocessed rsfMRI data (six head motion parameters; global signals from the CSF, WM, and the whole brain; motion outliers). We defined the head motion parameters from the estimates of the motion-correction step and the motion outliers as FD >0.5 mm or standardized DVARS (Power et al., 2014) >1.5 standard deviations (Parkes et al., 2018). DVARS was calculated according to a previous study (Power et al., 2014).

To investigate the FC of the NAcc and other striata, namely the

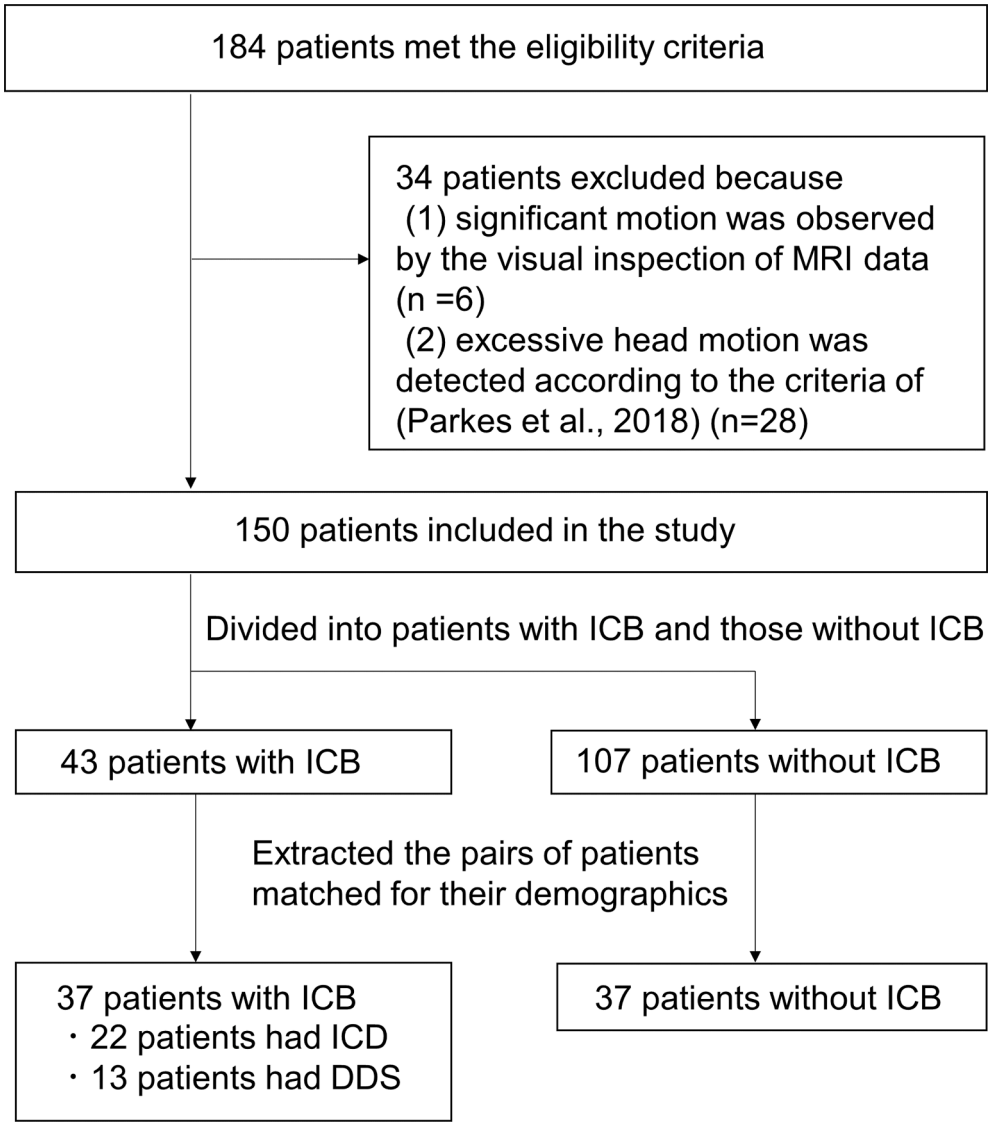

Fig. 1. Flowchart of our study. Thirty-seven patients with and without ICB were finally analyzed. Abbreviations: ICB, impulsive compulsive behaviors; ICD, impulse control disorders; DDS, dopamine dysregulation syndrome.

caudate and putamen, seed-based correlation analysis was conducted with Nilearn 0.8.1 (https://nilearn.github.io/stable/index.html). Six seeds (the right or left NAcc, putamen, and caudate) were used and defined using Harvard-Oxford cortical and subcortical structural atlases (Desikan et al., 2006). The FC between each seed and voxel in the whole brain was calculated using Fisher's z-transformed Pearson's correlation coefficient (z-value) while regressing out the nuisance signals described above.

To analyze GMV, T1-weighted data were preprocessed separately using Statistical Parametric Mapping 12 (SPM12) (Friston, 2003) on MATLAB R2020a (Mathworks, Natick, MA). Details of the preprocessing steps have been described in our previous study (Kajiyama et al., 2021). In brief, T1-weighted data were segmented into CSF, GM, and WM, spatially normalized to the MNI standard space and spatially smoothed with a Gaussian kernel of 8 mm FWHM.

2.8. Statistical analysis

To compare the basic and neuroimaging characteristics between the ICB and non-ICB groups, we first extracted pairs from the two groups matched for age, sex, disease duration, and LEDD of the DA. Disease duration and DA dose were used for extracting the pairs because both are major risk factors of ICB (Evans et al., 2009) and affect other non-motor symptoms.

To compare basic characteristics between the ICB and non-ICB groups, Mann–Whitney *U* tests were applied for continuous variables. For categorical variables, chi-squared tests were applied, and if the ratio of cells with an expected frequency <5 was >20 %, Fisher's exact tests were applied (Kim, 2017). These tests were performed using R (version 4.1.2, https://www.r-project.org/), and $P < 0.05$ was considered statistically significant.

A second-level general linear model analysis implemented in SPM12 was used to compare the FC on each seed or GMV between the ICB and non-ICB groups and between patients with ICD and those with DDS. To compare the ICB and non-ICB groups, we performed two-tailed *t*-tests for FC and an analysis of covariance for GMV, defining total brain volume (TBV) as covariates of no interest. To compare patients with ICD and DDS, two separate binary variables (i.e., whether they had ICD/DDS) were firstly regressed against FC or GMV within the ICB group, setting TBV as covariates of no interest in GMV. We then assessed the differences between the coefficients of ICD (ICD effect) and DDS (DDS effect) using a two-tailed *t*-test. A voxel-level uncorrected $P < 0.001$ and a cluster-wise family-wise error-corrected $P < 0.05$ were considered statistically significant.

To rule out the possibility of the involvement of possible confounders in each of the significant clusters, we calculated Spearman's correlation coefficients between the mean z-value of each significant cluster and each continuous variable in the basic characteristics. We also performed Mann–Whitney *U* tests on the mean z-value of each significant cluster divided by each categorical variable for the basic characteristics.

2.9. Data and code availability

Data from the clinical evaluations and codes used for this analysis are available at github. The raw MRI data is not openly available owing to privacy restrictions of clinical data. However, they are available upon a reasonable request to the corresponding authors.

3. Results

3.1. Basic characteristics

Among 150 eligible patients, we extracted 37 pairs of the ICB and non-ICB groups (Fig. 1). According to the J-QUIP, 22, 13, and 8 patients had ICD, DDS, and both, respectively. No significant differences in basic characteristics, including depression and cognitive function, were found between the ICB and non-ICB groups (Table 1; see Supplementary Tables 1 and 2 for the basic characteristics of the 150 eligible patients and patients with ICD or DDS, respectively).

3.2. Comparisons between the ICB and non-ICB groups

We first compared the FC for six seeds (the right or left NAcc, putamen and caudate) between the ICB and non-ICB groups. Comparisons concerning the FC of the right NAcc revealed that the FC of the ICB group was significantly lower in the bilateral ventromedial prefrontal cortex (vmPFC) than that of the non-ICB group (Fig. 1A; see Supplementary Table 3 for statistical values and peak MNI-coordinates on each significant cluster). The mean z-values of this significant cluster were 0.10 ± 0.10 and 0.25 ± 0.12 in the ICB and non-ICB groups, respectively (Fig. 1B). In contrast, the FC of the ICB group was significantly higher in the left middle occipital gyrus (MOG) than that of the non-ICB group (Fig. 1A). The mean z-values of FC in this cluster were 0.019 ± 0.083 and -0.090 ± 0.088 in the ICB and non-ICB groups, respectively (Fig. 1C). We observed no significant differences between the ICB and non-ICB groups regarding the FC in the left NAcc, bilateral caudate, or bilateral putamen and the GMV.

Table 1
Basic characteristics of patients with Parkinson's disease in the ICB and non-ICB groups.

Characteristics		ICB (n = 37)	non-ICB (n = 37)	*P*
Age (years)		66.0 (11.6)	66.6 (11.3)	0.79
Sex (male)		17 (46 %) †	18 (49 %) †	1.00 ‡
Handedness (right)		37 (100 %) †	34 (92 %) †	0.24 *
Dominant side of motor symptom	right	20 (54 %) †	12 (32 %) †	0.17 *
	left	14 (38 %) †	20 (54 %) †	
	no laterality	3 (8.1 %) †	5 (14 %) †	
Disease duration (years)		8.32 (8.1)	8.1 (7.0)	0.93
Medications (yes)	pramipexole	7 (19 %) †	10 (27 %) †	0.58 ‡
	ropinirole	6 (16 %) †	1 (2.7 %) †	0.11*
	rotigotine	9 (24 %) †	8 (22 %) †	1.00 ‡
LEDD (mg)	total	533.5 (441.0)	606.6 (585.6)	0.86
	DA	97.6 (124.2)	105.4 (139.8)	0.81
Apathy Scale		16.2 (8.3)	15.9 (6.8)	0.76
ESS		9.2 (4.2)	8.3 (5.4)	0.23
FAB		11.3 (6.7)	14.2 (2.7)	0.69
GDS		6.0 (3.3)	5.3 (3.0)	0.34
HAM-D		5.6 (4.6)	6.7 (4.9)	0.27
MMSE		26.7 (3.9)	27.6 (3.8)	0.13
PDQ-39		47.2 (22.1)	46.5 (28.0)	0.62
MDS-UPDRS	part1	11.5 (5.8)	10.8 (6.7)	0.59
	part2	15.6 (8.2)	15.3 (10.4)	0.64
	part3	31.4 (14.0)	31.2 (17.9)	0.67
	part4	3.9 (4.2)	3.4 (4.5)	0.36
J-QUIP	Total score	2.1 (2.1)	NaN	NaN
	A (score ≥ 1)	6 (16 %) †	NaN	NaN
	B (score ≥ 1)	3 (8.1 %) †	NaN	NaN
	C (score ≥ 1)	6 (16 %) †	NaN	NaN
	D (score ≥ 1)	12 (32 %) †	NaN	NaN
	E (score ≥ 1)	20 (54 %) †	NaN	NaN
	F (score ≥ 1)	13 (35 %) †	NaN	NaN

Scores are presented as the mean (SD). †Scores are presented as frequency (percentage). ‡ P-values were calculated using the chi-square test. * P-values were calculated using Fisher's exact test.
Abbreviations: ICB, impulsive compulsive behaviors; LEDD, levodopa equivalent daily dose; DA, dopamine agonist; ESS, Epworth Sleepiness Scale; FAB, Frontal Assessment Battery; GDS, Geriatric Depression Scale; HAM-D, Hamilton Depression Rating Scale; MMSE, Mini-Mental State Examination; PDQ-39, Parkinson's Disease Questionnaire-39 Summary Index; MDS-UPDRS, Movement Disorder Society-Sponsored Revision of the Unified Parkinson's Disease Rating Scale; J-QUIP, Japanese version of the Questionnaire for Impulsive Compulsive Disorders in Parkinson's Disease.

3.3. Comparisons between the ICD and DDS effects

We then compared the FC and GMV between patients with ICD and those with DDS. The FC of patients with ICD was lower between the right putamen and left superior temporal gyrus (STG) and between the left caudate and bilateral MOG than that of patients with DDS (Fig. 2A). The mean z-values of the FC between the right putamen and left STG were -0.041 ± 0.18, 0.12 ± 0.13, and 0.019 ± 0.12 in patients with ICD, those with DDS, and the non-ICB group, respectively (Fig. 2B). The mean z-values of the FC between the left caudate and bilateral MOG were -0.13 ± 0.089, 0.0025 ± 0.11, and -0.11 ± 0.093 in patients with ICD, those with DDS, and the non-ICB group, respectively (Fig. 2C). In contrast, the FC between the left NAcc and right posterior cingulate cortex (PCC) in patients with ICD was lower than that in patients with DDS (Fig. 2A). The mean z-values of the FC between the left NAcc and right PCC were 0.055 ± 0.12, -0.082 ± 0.10, and 0.029 ± 0.098 in patients with ICD, those with DDS, and the non-ICB group, respectively (Fig. 2D). Furthermore, we found no statistically significant differences between patients with ICD and those with DDS regarding the FC of the right caudate, right NAcc, or left putamen, and those regarding the

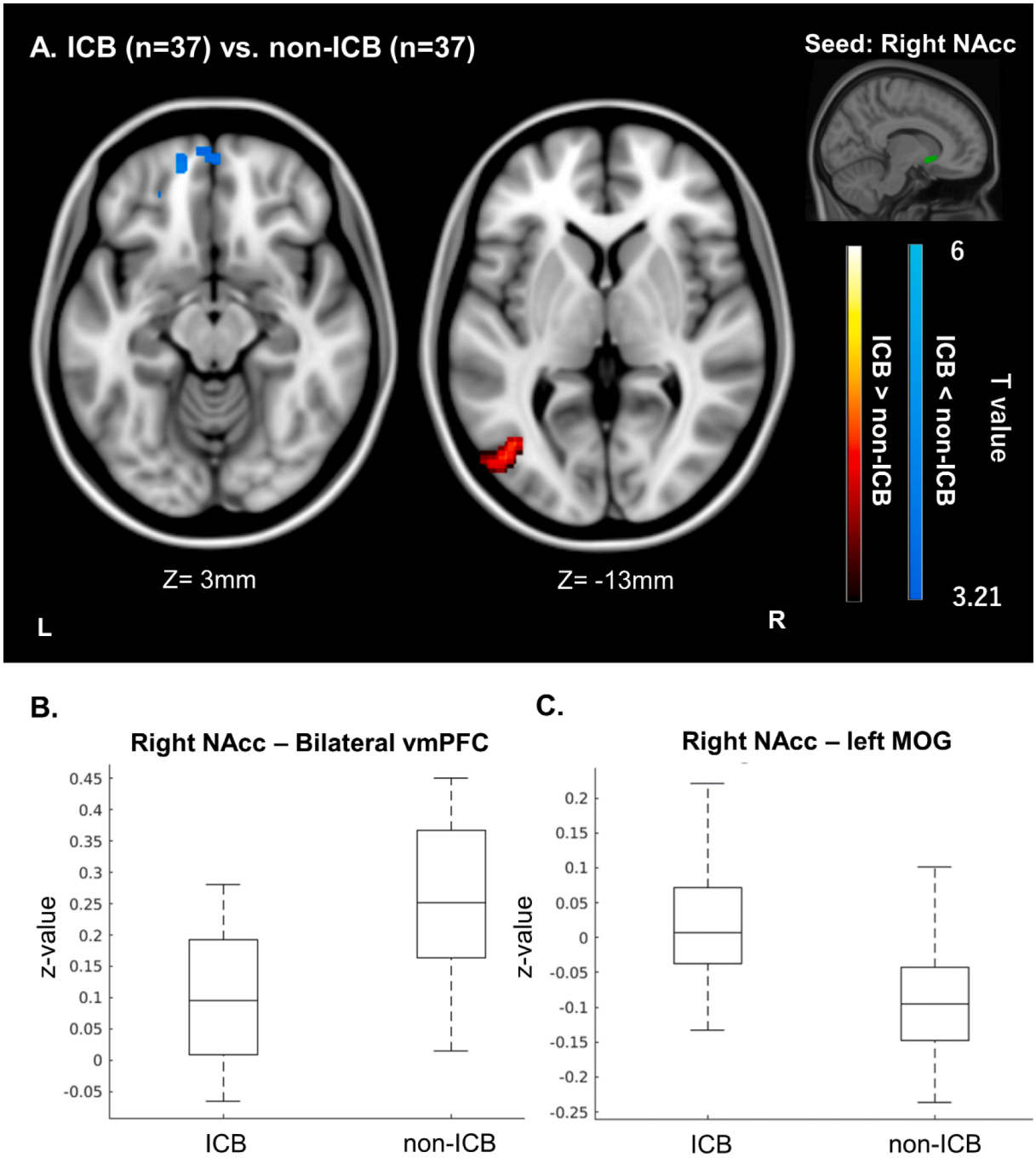

Fig. 2. Seed-based correlation analysis comparing the functional connectivity between the ICB and non-ICB groups. (A) The resulting spatial maps. The green-shaded region indicates the seed (right NAcc). The axial slices are displayed according to the neurological convention (left on the picture is left in the brain). (B, C) Boxplot of the mean Fisher-transformed Pearson's correlation coefficients (z-values) of each significant cluster in each group. (For interpretation of the references to color in this figure legend, the reader is referred to the web version of this article.) Abbreviations: ICB, impulsive compulsive behaviors; NAcc, nucleus accumbens; vmPFC, ventromedial prefrontal cortex; MOG, middle occipital gyrus.

GMV. Fig. 3.

3.4. Dependencies with possible confounding factors

We found no significant dependencies in the basic characteristics of the mean z-value of each significant cluster between the ICB and non-ICB groups (Supplementary Table 4) or between ICD and DDS effects (Supplementary Table 5).

4. Discussion

To the best of our knowledge, our study included the largest sample size to date of all related studies investigating ICB in PD (Santangelo et al., 2019). Here, we found that the FC of the right NAcc differed between the ICB and non-ICB groups and that the FC of the left NAcc, left caudate, and right putamen were altered in patients with ICD and those with DDS. None of these significant clusters was dependent on any other

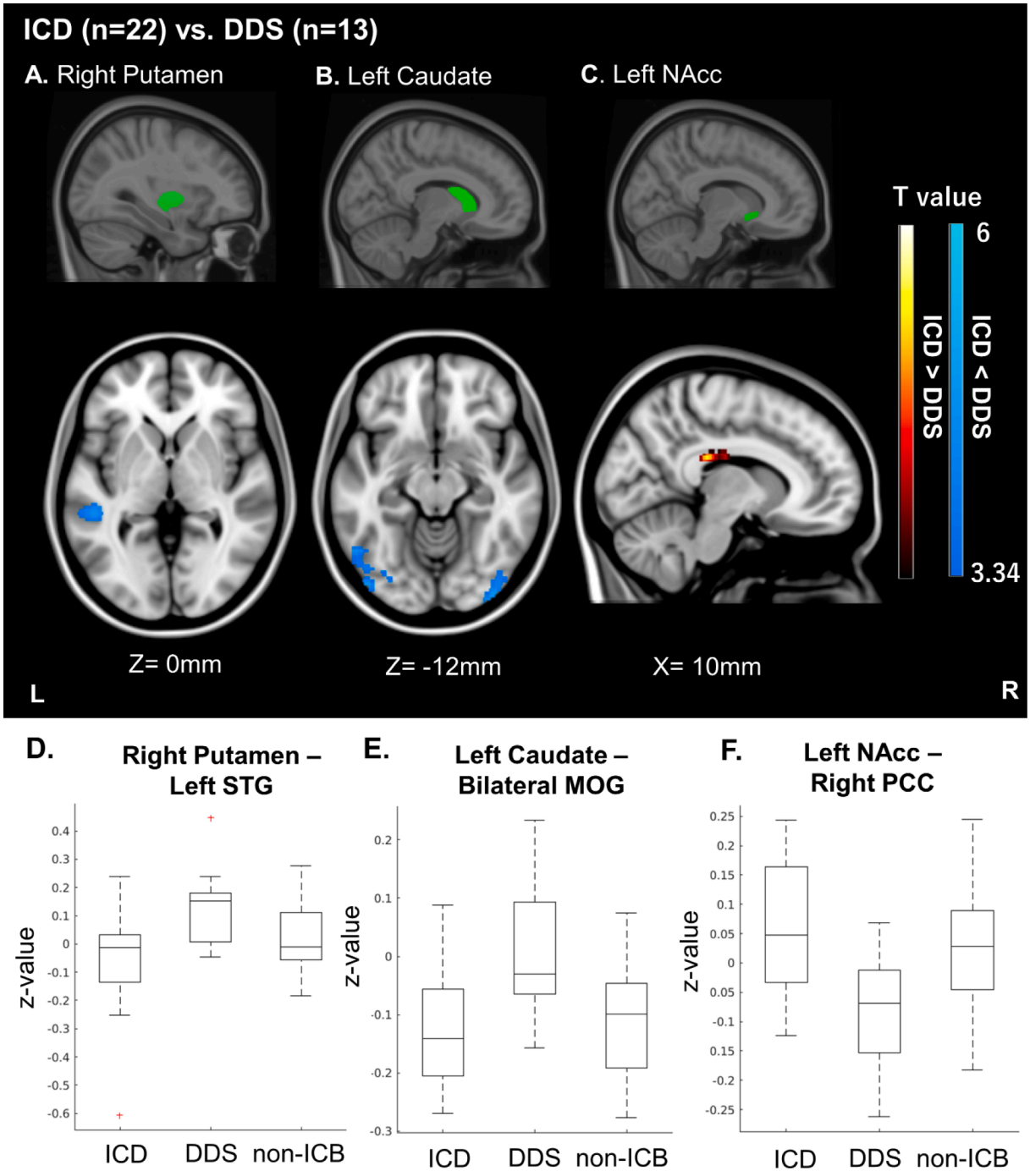

Fig. 3. Seed-based correlation analysis comparing the functional connectivity between the ICD and DDS effects in patients with PD. The resulting spatial maps using (A) right putamen, (B) left caudate, and (C) left NAcc as a seed. The green-shaded regions indicate the seed. The axial slices are displayed according to the neurological convention (left on the picture is left in the brain). (D – F) Boxplots of the mean z-value of each significant cluster in patients with ICD, those with DDS, and those without ICB, respectively. A red cross indicates an outlier detected by the default settings of "boxplot" in MATLAB. (For interpretation of the references to color in this figure legend, the reader is referred to the web version of this article.) Abbreviations: ICD, impulse control disorder; DDS, dopamine dysregulation syndrome; ICB, impulsive compulsive behaviors; PD, Parkinson's disease; STG, superior temporal gyrus; MOG, middle occipital gyrus; NAcc, nucleus accumbens; PCC, posterior cingulate cortex.

clinical demographics, suggesting that these differences were specifically derived from differences in ICB characteristics.

4.1. FC of the right NAcc was altered in the ICB group

The FC between the right NAcc and bilateral vmPFC was lower in the ICB group than in the non-ICB group, whereas the FC between the right NAcc and left MOG was higher in the ICB group. Several neuroimaging studies have revealed increased NAcc activity in patients with ICB (Santangelo et al., 2019). One study reported that fluorodopa uptake in patients with ICB was increased in the medial regions of the prefrontal cortex (Joutsa et al., 2012). Our data, combined with these results, suggest that the NAcc and vmPFC are functionally altered in patients with ICB, which is consistent with our finding that the FC between these two regions is decreased. Moreover, the vmPFC is structurally and functionally linked to the NAcc through the direct projections of glutamatergic neurons (Rusche et al., 2021; Wichmann and Delong, 2006). Previous neuroimaging studies have shown that the NAcc has a broad function in reward-based learning and the vmPFC plays a specific role in evaluating reward value (Haber and Knutson, 2010; Liu et al., 2011). These studies suggest that reduced FC between these regions can disrupt the transferring of precise reward values estimated from the vmPFC, and therefore, it might exaggerate the reward value of each outcome (Santangelo et al., 2019). Supporting this, one study revealed that patients with PD were hypersensitive to rewards during the Iowa Gambling Task (Kobayakawa et al., 2010). Nevertheless, further studies are needed to verify whether the decrease in FC between these two regions increases the valence of reward in each outcome.

The other explanation for why the decrease in FC between the right NAcc and vmPFC causes ICB is that the disconnection between the vmPFC and NAcc may disable learning from negative outcomes. One study revealed that patients with vmPFC lesions could not acquire Pavlovian threat conditioning (Battaglia et al., 2020), suggesting that the dysregulation of vmPFC might disrupt fear conditioning. Other studies have also reported that the vmPFC is crucial for risky decision-making (Clark, 2010; Rogalsky et al., 2012). Supporting these findings, patients with PD were less likely to learn from negative outcomes when dopaminergic drugs were effective than when these drugs were ineffective (Bódi et al., 2009; Frank et al., 2004), implying that dopaminergic drugs might disrupt learning from negative outcomes. Therefore, the overestimation of reward value on each outcome or the inability to learn from negative outcomes might lead to ICB.

We also observed a significant increase in FC between the right NAcc and left MOG in the ICB group. This is important as MOG plays a critical role in visual processing (Wang et al., 2015). Although there is no evidence that the decline in visual function is linked to ICB in PD, previous studies have implied that visuo-perceptual impairment is associated with decreased GMV (Garcia-Diaz et al., 2018; Pereira et al., 2009) and functional alteration of MOG in patients with PD (Li et al., 2020; Wang et al., 2022). Some task fMRI studies reported increased MOG cerebral blood flow in response to sexual visual cues in PD patients with hypersexuality (Politis et al., 2013) and higher activity in the ventral striatum following exposure to an image of a drug in patients with DDS compared with those without DDS (Evans et al., 2006; Loane et al., 2015). Another study suggested that structural changes in the WM of patients with ICB are related to visual and emotional processing and the reward system (Takeshige-Amano et al., 2022). Therefore, the functional alteration of MOG may affect the reward system in PD. Although speculative, our results suggest that the occipito-striatum network change might be associated with ICB in PD. Further neuropsychological and task-based fMRI assessments are needed to validate this finding.

No significant difference in the FC between the putamen and caudate was found. The reason for this specificity might be that the NAcc in patients with ICB was relatively intact compared with other subregions of the striatum. The load of alpha-synuclein in the NAcc was lower in patients with ICB than in those without ICB, whereas that in the putamen or caudate was not significantly different (Barbosa et al., 2019). Furthermore, the ventral striatum was relatively intact compared to other regions of the striatum until the late stage of PD (Cools, 2006). In contrast, some studies suggested the importance of the caudate and putamen in ICB in PD (Carriere et al., 2015; Gu et al., 2022; Ruitenberg et al., 2018). The dorsal striatum is structurally connected to the NAcc (Baydin et al., 2016; Powell and Leman, 1976) and is also involved in reward-based learning (Haber and Knutson, 2010). Moreover, this region is proposed to play a critical role in controlling habitual behavior (Burton et al., 2015) and impulsivity (Kim and Im, 2019). Therefore, altered dorsal striatum activity might also cause ICB. In summary, the NAcc and dorsal striatum are inter-connected, and their combined activity might contribute to ICB. Future studies are needed to clarify the specific role of each region in ICB.

4.2. FC of the striatum differed between patients with ICD and DDS

We observed a decrease in FC between the left NAcc and right PCC in patients with DDS compared with those with ICD. The PCC and NAcc play critical roles in reward-based learning (Liu et al., 2011). The decrease in FC in these regions reflects that the reward-processing steps are differentially altered in patients with ICD and DDS. Another reason for the decrease in FC between the right PCC and left NAcc in patients with DDS may be the difference in the sensitivity to levodopa between patients with ICD and those with DDS. Several case reports have indicated that levodopa can trigger DDS, whereas other DAs are apt to induce ICD (Evans et al., 2009). Moreover, one study reported that levodopa decreased the FC between the ventral striatum and PCC (Kelly et al., 2009), suggesting that the decrease in FC between these two regions in our results may reflect the effect of levodopa in patients with DDS. Therefore, patients with DDS might be more sensitive to levodopa than those with ICD.

We found statistically significant differences between patients with ICD and DDS in the cortico-dorsal striatal network, specifically in the FC between the right putamen and left STG and between the left caudate and bilateral MOG. The left STG is the main component of the language network, and several studies suggested that language function can be disrupted in patients with PD (Roheger et al., 2018). Several studies have also revealed that language processing was disrupted in patients with addictive behavior (Conversano et al., 2012; Darnai et al., 2022; Mlinarics et al., 2009). Therefore, we speculate that the increase in FC between the right putamen and left STG might reflect the underlying relationship between language function and addiction in DDS. However, it should be carefully considered whether DDS in PD can be considered in the same way as the addictive behavior in psychiatric disorders.

We also observed an increase in the FC between the left caudate and bilateral MOG in patients with DDS compared with those with ICD. As mentioned above, while the MOG can be structurally and functionally altered in PD, its relationship with ICB in PD remains unclear. In the context of dopaminergic sensitivity, levodopa improves low-level visual functions, such as color recognition (Büttner et al., 1994) and contrast sensitivity (Bulens et al., 1987), as well as aberrant visual evoked potentials in patients with PD (Bodis-Wollner and Yahr, 1978). Another study also reported that levodopa modulated the FC between the dorsal striatum and occipital regions (Kelly et al., 2009). These results suggest that levodopa alters visual functions. The caudate is also affected by dopaminergic stimuli, and several studies showed that this region contributes to the reward-based reaction to visual information in primates (Amita et al., 2020; Doi et al., 2020) and patients with PD (Stark et al., 2018). Moreover, levodopa administration affects the broad cortico-striatal network in PD (Ballarini et al., 2018; Shine et al., 2019; Yang et al., 2016). Considering that levodopa can trigger DDS, dopamine-induced network changes might be the underlying cause of DDS. Taken together, we speculate that the alteration of the reward system and the sensitivity to levodopa might be associated with the different network alterations in ICD and DDS. Our findings may explain ICB

heterogeneity, although insights about the network basis for the dopaminergic effect on ICD and DDS are needed.

4.3. No significant difference was found in the GMV

While we found significant differences in the FC of the striatum according to ICB features, we detected no significant differences in the GMV. While several previous studies also found no differences, other studies and *meta*-analyses suggest structural differences in the GM between patients with ICB and those without ICB (Gu et al., 2022; Santangelo et al., 2019). ICB are reversible symptoms since they can be ameliorated by reducing the dose of DA (Evans et al., 2009). This implies that reversible functional alterations can induce ICB, and our results suggest that functional differences can occur in patients with ICB, even without structural differences. Taken together, functional measurements can be more useful than structural measurements for detecting ICB, ICD, and DDS.

4.4. Limitations

This study has several limitations. First, we defined ICB using only the J-QUIP. The accuracy of J-QUIP in detecting ICB was comparable to that of an internationally established questionnaire for detecting ICB (Tanaka et al., 2013). Nevertheless, these scores are subjective and may underestimate the status of ICB (Perez-Lloret et al., 2012). Another drawback of J-QUIP is that this measurement has not been validated for assessing the severity of ICB (Evans et al., 2019). Hence, we could not examine the correlation between the severity of ICB and the neuroimaging metrics. Therefore, future studies are required to evaluate the status of ICB using objective neuropsychological tests, such as the Iowa Gambling Task (Buelow and Suhr, 2009), and measurements assessing the severity of ICB (Takahashi et al., 2022).

Second, this is a retrospective study, therefore, whether DRT induced alterations in FC or they already existed before DRT is unclear. Hence, future prospective and longitudinal studies are required to reveal the causality of changes in FC in these significantly different clusters.

Third, the number of patients within some ICB subcategories, such as pathological gambling or hypersexuality, was relatively small. Therefore, we could not differentiate the neural correlates of each ICB subcategory. Though previous neuroimaging studies have also not distinguished these subcategories (Santangelo et al., 2019), the neural correlates might differ across them (Weintraub and Claassen, 2017). Therefore, future large population studies are required to detect the unique neural characteristics of each ICB subcategory.

4.5. Conclusions

Our findings showed that cortico-striatal networks play an important role in ICB and that these networks reflect the different characteristics of ICD and DDS. Evaluating the FC of these networks might be useful for detecting ICB, which may be underestimated through clinical interviews alone. Elucidating the altered regions is important for identifying biomarkers for ICB and clarifying the treatment target of ICB with neuromodulation.

Declaration of Competing Interest

The authors declare that they have no known competing financial interests or personal relationships that could have appeared to influence the work reported in this paper.

Data availability

Data will be made available on request.

Acknowledgements

This study was supported by Grants-in-Aid from the Research Committee of Central Nervous System Degenerative Diseases, Research on Policy Planning and Evaluation for Rare and Intractable Diseases, Health, Labor and Welfare Sciences Research Grants, the Ministry of Health, Labor and Welfare, Japan (Grant number: 20FC1049).

Appendix A. Supplementary data

Supplementary data to this article can be found online at https://doi.org/10.1016/j.nicl.2022.103307.

References

Amita, H., Kim, H.F., Inoue, K.-I., Takada, M., Hikosaka, O., 2020. Optogenetic manipulation of a value-coding pathway from the primate caudate tail facilitates saccadic gaze shift. Nat. Commun. 11, 1876. https://doi.org/10.1038/s41467-020-15802-y.

Ballarini, T., Růžička, F., Bezdicek, O., Růžička, E., Roth, J., Villringer, A., Vymazal, J., Mueller, K., Schroeter, M.L., Jech, R., 2018. Unraveling connectivity changes due to dopaminergic therapy in chronically treated Parkinson's disease patients. Sci. Rep. 8, 14328. https://doi.org/10.1038/s41598-018-31988-0.

Barbosa, P., Hapuarachchi, B., Djamshidian, A., Strand, K., Lees, A.J., de Silva, R., Holton, J.L., Warner, T.T., 2019. Lower nucleus accumbens α-synuclein load and D3 receptor levels in Parkinson's disease with impulsive compulsive behaviours. Brain 142, 3580–3591. https://doi.org/10.1093/brain/awz298.

Battaglia, S., Garofalo, S., di Pellegrino, G., Starita, F., 2020. Revaluing the role of vmPFC in the acquisition of pavlovian threat conditioning in humans. J. Neurosci. 40, 8491–8500. https://doi.org/10.1523/JNEUROSCI.0304-20.2020.

Baydin, S., Yagmurlu, K., Tanriover, N., Gungor, A., Rhoton Jr, A.L., 2016. Microsurgical and Fiber Tract Anatomy of the Nucleus Accumbens. Oper Neurosurg (Hagerstown) 12, 269–288. https://doi.org/10.1227/NEU.0000000000001133.

Bódi, N., Kéri, S., Nagy, H., Moustafa, A., Myers, C.E., Daw, N., Dibó, G., Takáts, A., Bereczki, D., Gluck, M.A., 2009. Reward-learning and the novelty-seeking personality: a between- and within-subjects study of the effects of dopamine agonists on young Parkinson's patients. Brain 132, 2385–2395. https://doi.org/10.1093/brain/awp094.

Bodis-Wollner, I., Yahr, M.D., 1978. Measurements of visual evoked potentials in Parkinson's disease. Brain 101, 661–671. https://doi.org/10.1093/brain/101.4.661.

Buelow, M.T., Suhr, J.A., 2009. Construct validity of the Iowa Gambling Task. Neuropsychol. Rev. 19, 102–114. https://doi.org/10.1007/s11065-009-9083-4.

Bulens, C., Meerwaldt, J.D., Van der Wildt, G.J., Van Deursen, J.B., 1987. Effect of levodopa treatment on contrast sensitivity in Parkinson's disease. Ann. Neurol. 22, 365–369. https://doi.org/10.1002/ana.410220313.

Burton, A.C., Nakamura, K., Roesch, M.R., 2015. From ventral-medial to dorsal-lateral striatum: neural correlates of reward-guided decision-making. Neurobiol. Learn. Mem. 117, 51–59. https://doi.org/10.1016/j.nlm.2014.05.003.

Büttner, T., Kuhn, W., Patzold, T., Przuntek, H., 1994. L-Dopa improves colour vision in Parkinson's disease. J. Neural Transm. Park. Dis. Dement. Sect. 7, 13–19. https://doi.org/10.1007/BF02252659.

Carriere, N., Lopes, R., Defebvre, L., Delmaire, C., Dujardin, K., 2015. Impaired corticostriatal connectivity in impulse control disorders in Parkinson disease. Neurology 84, 2116–2123. https://doi.org/10.1212/WNL.0000000000001619.

Clark, L., 2010. Decision-making during gambling: an integration of cognitive and psychobiological approaches. Philos. Trans. R. Soc. Lond. B Biol. Sci. 365, 319–330. https://doi.org/10.1098/rstb.2009.0147.

Conversano, C., Marazziti, D., Carmassi, C., Baldini, S., Barnabei, G., Dell'Osso, L., 2012. Pathological gambling: a systematic review of biochemical, neuroimaging, and neuropsychological findings. Harv. Rev. Psychiatry 20, 130–148. https://doi.org/10.3109/10673229.2012.694318.

Cools, R., 2006. Dopaminergic modulation of cognitive function-implications for L-DOPA treatment in Parkinson's disease. Neurosci. Biobehav. Rev. 30, 1–23. https://doi.org/10.1016/j.neubiorev.2005.03.024.

Darnai, G., Perlaki, G., Orsi, G., Arató, Á., Szente, A., Horváth, R., Áfra, E., Nagy, S.A., Kovács, N., Dóczi, T., Janszky, J., 2022. Language processing in Internet use disorder: Task-based fMRI study. PLoS One 17, e0269979.

Desikan, R.S., Ségonne, F., Fischl, B., Quinn, B.T., Dickerson, B.C., Blacker, D., Buckner, R.L., Dale, A.M., Maguire, R.P., Hyman, B.T., Albert, M.S., Killiany, R.J., 2006. An automated labeling system for subdividing the human cerebral cortex on MRI scans into gyral based regions of interest. Neuroimage 31, 968–980. https://doi.org/10.1016/j.neuroimage.2006.01.021.

Dodd, M.L., Klos, K.J., Bower, J.H., Geda, Y.E., Josephs, K.A., Ahlskog, J.E., 2005. Pathological gambling caused by drugs used to treat Parkinson disease. Arch. Neurol. 62, 1377–1381. https://doi.org/10.1001/archneur.62.9.noc50009.

Doi, T., Fan, Y., Gold, J.I., Ding, L., 2020. The caudate nucleus contributes causally to decisions that balance reward and uncertain visual information. Elife 9. https://doi.org/10.7554/eLife.56694.

Esteban, O., Markiewicz, C.J., Blair, R.W., Moodie, C.A., Isik, A.I., Erramuzpe, A., Kent, J. D., Goncalves, M., DuPre, E., Snyder, M., Oya, H., Ghosh, S.S., Wright, J., Durnez, J., Poldrack, R.A., Gorgolewski, K.J., 2019. fMRIPrep: a robust preprocessing pipeline

for functional MRI. Nat. Methods 16, 111–116. https://doi.org/10.1038/s41592-018-0235-4.
Evans, A.H., Okai, D., Weintraub, D., Lim, S.-Y., O'Sullivan, S.S., Voon, V., Krack, P., Sampaio, C., Post, B., Leentjens, A.F.G., Martinez-Martin, P., Stebbins, G.T., Goetz, C. G., Schrag, A., Members of the International Parkinson and Movement Disorder Society (IPMDS) Rating Scales Review Committee, 2019. Scales to assess impulsive and compulsive behaviors in Parkinson's disease: critique and recommendations. Mov. Disord. 34, 791–798. 10.1002/mds.27689.
Evans, A.H., Pavese, N., Lawrence, A.D., Tai, Y.F., Appel, S., Doder, M., Brooks, D.J., Lees, A.J., Piccini, P., 2006. Compulsive drug use linked to sensitized ventral striatal dopamine transmission. Ann. Neurol. 59, 852–858. https://doi.org/10.1002/ana.20822.
Evans, A.H., Strafella, A.P., Weintraub, D., Stacy, M., 2009. Impulsive and compulsive behaviors in Parkinson's disease. Mov. Disord. 24, 1561–1570. https://doi.org/10.1002/mds.22505.
Frank, M.J., Seeberger, L.C., O'reilly, R.C., 2004. By carrot or by stick: cognitive reinforcement learning in parkinsonism. Science 306, 1940–1943. https://doi.org/10.1126/science.1102941.
Friston, K.J., 2003. Statistical Parametric Mapping. In: Kötter, R. (Ed.), Neuroscience DAtAbAses: A PrActicAl Guide. Springer, US, Boston, MA, pp. 237–250. https://doi.org/10.1007/978-1-4615-1079-6_16.
Garcia-Diaz, A.I., Segura, B., Baggio, H.C., Marti, M.J., Valldeoriola, F., Compta, Y., Bargallo, N., Uribe, C., Campabadal, A., Abos, A., Junque, C., 2018. Structural brain correlations of visuospatial and visuoperceptual tests in Parkinson's disease. J. Int. Neuropsychol. Soc. 24, 33–44. https://doi.org/10.1017/S1355617717000583.
Garcia-Ruiz, P.J., Martinez Castrillo, J.C., Alonso-Canovas, A., Herranz Barcenas, A., Vela, L., Sanchez Alonso, P., Mata, M., Olmedilla Gonzalez, N., Mahillo Fernandez, I., 2014. Impulse control disorder in patients with Parkinson's disease under dopamine agonist therapy: a multicentre study. J. Neurol. Neurosurg. Psychiatry 85, 840–844. https://doi.org/10.1136/jnnp-2013-306787.
Gatto, E.M., Aldinio, V., 2019. Impulse control disorders in Parkinson's disease. A brief and comprehensive review. Front. Neurol. 10, 351. https://doi.org/10.3389/fneur.2019.00351.
Gu, L., Shu, H., Wang, Y., Xu, H., 2022. Exploring brain changes of impulse control disorders in Parkinson's disease: An ALE study. Front. Aging Neurosci. 14, 966525 https://doi.org/10.3389/fnagi.2022.966525.
Haber, S.N., Knutson, B., 2010. The reward circuit: linking primate anatomy and human imaging. Neuropsychopharmacology 35, 4–26. https://doi.org/10.1038/npp.2009.129.
Joutsa, J., Martikainen, K., Niemelä, S., Johansson, J., Forsback, S., Rinne, J.O., Kaasinen, V., 2012. Increased medial orbitofrontal [18F]fluorodopa uptake in Parkinsonian impulse control disorders. Mov. Disord. 27, 778–782. https://doi.org/10.1002/mds.24941.
Kajiyama, Y., Hattori, N., Nakano, T., Revankar, G.S., Otomune, H., Hashimoto, R., Mori, E., Ikeda, M., Mihara, M., Mochizuki, H., 2021. Decreased frontotemporal connectivity in patients with parkinson's disease experiencing face pareidolia. NPJ Parkinsons Dis 7, 90. https://doi.org/10.1038/s41531-021-00237-z.
Kanai, R., Rees, G., 2011. The structural basis of inter-individual differences in human behaviour and cognition. Nat. Rev. Neurosci. 12, 231–242. https://doi.org/10.1038/nrn3000.
Kelly, C., de Zubicaray, G., Di Martino, A., Copland, D.A., Reiss, P.T., Klein, D.F., Castellanos, F.X., Milham, M.P., McMahon, K., 2009. L-dopa modulates functional connectivity in striatal cognitive and motor networks: a double-blind placebo-controlled study. J. Neurosci. 29, 7364–7378. https://doi.org/10.1523/JNEUROSCI.0810-09.2009.
Kim, H.Y., 2017. Statistical notes for clinical researchers: chi-squared test and Fisher's exact test. Restor. Dent. Endod. 42, 152–155. https://doi.org/10.5395/rde.2017.42.2.152.
Kim, B., Im, H.I., 2019. The role of the dorsal striatum in choice impulsivity. Ann. N. Y. Acad. Sci. 1451, 92–111. https://doi.org/10.1111/nyas.13961.
Kobayakawa, M., Tsuruya, N., Kawamura, M., 2010. Sensitivity to reward and punishment in Parkinson's disease: an analysis of behavioral patterns using a modified version of the Iowa Gambling Task. Parkinsonism Relat. Disord. 16, 453–457. https://doi.org/10.1016/j.parkreldis.2010.04.011.
Koike, S., Tanaka, S.C., Okada, T., Aso, T., Yamashita, A., Yamashita, O., Asano, M., Maikusa, N., Morita, K., Okada, N., Fukunaga, M., Uematsu, A., Togo, H., Miyazaki, A., Murata, K., Urushibata, Y., Autio, J., Ose, T., Yoshimoto, J., Araki, T., Glasser, M.F., Van Essen, D.C., Maruyama, M., Sadato, N., Kawato, M., Kasai, K., Okamoto, Y., Hanakawa, T., Hayashi, T., 2021. Brain/MINDS beyond human brain MRI project: A protocol for multi-level harmonization across brain disorders throughout the lifespan. NeuroImage Clin. 30, 102600 https://doi.org/10.1016/j.nicl.2021.102600.
Lawrence, A.D., Evans, A.H., Lees, A.J., 2003. Compulsive use of dopamine replacement therapy in Parkinson's disease: reward systems gone awry? Lancet Neurol. 2, 595–604. https://doi.org/10.1016/s1474-4422(03)00529-5.
Li, M.G., He, J.F., Liu, X.Y., Wang, Z.F., Lou, X., Ma, L., 2020. Structural and Functional Thalamic Changes in Parkinson's Disease With Mild Cognitive Impairment. J Magn Reson Imaging 52, 1207–1215. https://doi.org/10.1002/jmri.27195.
Liu, X., Hairston, J., Schrier, M., Fan, J., 2011. Common and distinct networks underlying reward valence and processing stages: a meta-analysis of functional neuroimaging studies. Neurosci. Biobehav. Rev. 35, 1219–1236. https://doi.org/10.1016/j.neubiorev.2010.12.012.
Loane, C., Wu, K., O'Sullivan, S.S., Lawrence, A.D., Woodhead, Z., Lees, A.J., Piccini, P., Politis, M., 2015. Psychogenic and neural visual-cue response in PD dopamine dysregulation syndrome. Parkinsonism Relat. Disord. 21, 1336–1341. https://doi.org/10.1016/j.parkreldis.2015.09.042.
Marek, S., Tervo-Clemmens, B., Calabro, F.J., Montez, D.F., Kay, B.P., Hatoum, A.S., Donohue, M.R., Foran, W., Miller, R.L., Hendrickson, T.J., Malone, S.M., Kandala, S., Feczko, E., Miranda-Dominguez, O., Graham, A.M., Earl, E.A., Perrone, A.J., Cordova, M., Doyle, O., Moore, L.A., Conan, G.M., Uriarte, J., Snider, K., Lynch, B.J., Wilgenbusch, J.C., Pengo, T., Tam, A., Chen, J., Newbold, D.J., Zheng, A., Seider, N. A., Van, A.N., Metoki, A., Chauvin, R.J., Laumann, T.O., Greene, D.J., Petersen, S.E., Garavan, H., Thompson, W.K., Nichols, T.E., Yeo, B.T.T., Barch, D.M., Luna, B., Fair, D.A., Dosenbach, N.U.F., 2022. Reproducible brain-wide association studies require thousands of individuals. Nature 603, 654–660. https://doi.org/10.1038/s41586-022-04492-9.
Mata-Marín, D., Pineda-Pardo, J.A., Molina, J.A., Vela, L., Alonso-Frech, F., Obeso, I., 2021. Aberrant salient and corticolimbic connectivity in hypersexual Parkinson's disease. Brain Connectivity. https://doi.org/10.1089/brain.2020.0868.
Mlinarics, R., Kelemen, O., Sefcsik, T., Németh, D., 2009. Cognitive impairment in patients with alcoholism after long-term abstinence. Neuropsychopharmacol. Hung. 11, 135–139.
Nakano, T., Kajiyama, Y., Revankar, G.S., Hashimoto, R., Watanabe, Y., Kishima, H., Ikeda, M., Mihara, M., Mochizuki, H., Hattori, N., 2021. Neural networks associated with quality of life in patients with Parkinson's disease. Parkinsonism Relat. Disord. 89, 6–12. https://doi.org/10.1016/j.parkreldis.2021.06.007.
Navalpotro-Gomez, I., Kim, J., Paz-Alonso, P.M., Delgado-Alvarado, M., Quiroga-Varela, A., Jimenez-Urbieta, H., Carreiras, M., Strafella, A.P., Rodriguez-Oroz, M.C., 2020. Disrupted salience network dynamics in Parkinson's disease patients with impulse control disorders. Parkinsonism Relat. Disord. 70, 74–81. https://doi.org/10.1016/j.parkreldis.2019.12.009.
Otomune, H., Mihara, M., Hattori, N., Fujimoto, H., Kajiyama, Y., Konaka, K., Mitani, Y., Watanabe, Y., Mochizuki, H., 2019. Involvement of cortical dysfunction in frequent falls in patients with Parkinson's disease. Parkinsonism Relat. Disord. 64, 169–174. https://doi.org/10.1016/j.parkreldis.2019.04.007.
Parkes, L., Fulcher, B., Yücel, M., Fornito, A., 2018. An evaluation of the efficacy, reliability, and sensitivity of motion correction strategies for resting-state functional MRI. Neuroimage 171, 415–436. https://doi.org/10.1016/j.neuroimage.2017.12.073.
Pereira, J.B., Junqué, C., Martí, M.-J., Ramirez-Ruiz, B., Bargalló, N., Tolosa, E., 2009. Neuroanatomical substrate of visuospatial and visuoperceptual impairment in Parkinson's disease. Mov. Disord. 24, 1193–1199. https://doi.org/10.1002/mds.22560.
Perez-Lloret, S., Rey, M.V., Fabre, N., Ory, F., Spampinato, U., Montastruc, J.-L., Rascol, O., 2012. Do Parkinson's disease patients disclose their adverse events spontaneously? Eur. J. Clin. Pharmacol. 68, 857–865. https://doi.org/10.1007/s00228-011-1198-x.
Politis, M., Loane, C., Wu, K., O'Sullivan, S.S., Woodhead, Z., Kiferle, L., Lawrence, A.D., Lees, A.J., Piccini, P., 2013. Neural response to visual sexual cues in dopamine treatment-linked hypersexuality in Parkinson's disease. Brain 136, 400–411. https://doi.org/10.1093/brain/aws326.
Postuma, R.B., Berg, D., Stern, M., Poewe, W., Olanow, C.W., Oertel, W., Obeso, J., Marek, K., Litvan, I., Lang, A.E., Halliday, G., Goetz, C.G., Gasser, T., Dubois, B., Chan, P., Bloem, B.R., Adler, C.H., Deuschl, G., 2015. MDS clinical diagnostic criteria for Parkinson's disease. Mov. Disord. 30, 1591–1601. https://doi.org/10.1002/mds.26424.
Powell, E.W., Leman, R.B., 1976. Connections of the nucleus accumbens. Brain Res. 105, 389–403. https://doi.org/10.1016/0006-8993(76)90589-8.
Power, J.D., Mitra, A., Laumann, T.O., Snyder, A.Z., Schlaggar, B.L., Petersen, S.E., 2014. Methods to detect, characterize, and remove motion artifact in resting state fMRI. Neuroimage 84, 320–341. https://doi.org/10.1016/j.neuroimage.2013.08.048.
Rocha, E.M., De Miranda, B., Sanders, L.H., 2018. Alpha-synuclein: Pathology, mitochondrial dysfunction and neuroinflammation in Parkinson's disease. Neurobiol. Dis. 109, 249–257. https://doi.org/10.1016/j.nbd.2017.04.004.
Rogalsky, C., Vidal, C., Li, X., Damasio, H., 2012. Risky decision-making in older adults without cognitive deficits: an fMRI study of VMPFC using the Iowa Gambling Task. Soc. Neurosci. 7, 178–190. https://doi.org/10.1080/17470919.2011.588340.
Roheger, M., Kalbe, E., Liepelt-Scarfone, I., 2018. Progression of cognitive decline in Parkinson's disease. J. Parkinsons. Dis. 8, 183–193. https://doi.org/10.3233/JPD-181306.
Ruitenberg, M.F.L., Wu, T., Averbeck, B.B., Chou, K.L., Koppelmans, V., Seidler, R.D., 2018. Impulsivity in Parkinson's disease is associated with alterations in affective and sensorimotor striatal networks. Front. Neurol. 9, 279. https://doi.org/10.3389/fneur.2018.00279.
Rusche, T., Kaufmann, J., Voges, J., 2021. Nucleus accumbens projections: Validity and reliability of fiber reconstructions based on high-resolution diffusion-weighted MRI. Hum. Brain Mapp. 42, 5888–5910. https://doi.org/10.1002/hbm.25657.
Santangelo, G., Raimo, S., Cropano, M., Vitale, C., Barone, P., Trojano, L., 2019. Neural bases of impulse control disorders in Parkinson's disease: A systematic review and an ALE meta-analysis. Neurosci. Biobehav. Rev. 107, 672–685. https://doi.org/10.1016/j.neubiorev.2019.09.041.
Shine, J.M., Bell, P.T., Matar, E., Poldrack, R.A., Lewis, S.J.G., Halliday, G.M., O'Callaghan, C., 2019. Dopamine depletion alters macroscopic network dynamics in Parkinson's disease. Brain 142, 1024–1034. https://doi.org/10.1093/brain/awz034.
Stark, A.J., Smith, C.T., Lin, Y.-C., Petersen, K.J., Trujillo, P., van Wouwe, N.C., Kang, H., Donahue, M.J., Kessler, R.M., Zald, D.H., Claassen, D.O., 2018. Nigrostriatal and mesolimbic D2/3 receptor expression in Parkinson's disease patients with compulsive reward-driven behaviors. J. Neurosci. 38, 3230–3239. https://doi.org/10.1523/JNEUROSCI.3082-17.2018.
Takahashi, M., Koh, J., Yorozu, S., Kajimoto, Y., Nakayama, Y., Sakata, M., Yasui, M., Hiwatani, Y., Weintraub, D., Ito, H., 2022. Validation of the Japanese version of the Questionnaire for Impulsive-Compulsive Disorders in Parkinson's Disease-Rating

Scale (QUIP-RS). Parkinsons Dis. 2022, 1503167. https://doi.org/10.1155/2022/1503167.

Takeshige-Amano, H., Hatano, T., Kamagata, K., Andica, C., Uchida, W., Abe, M., Ogawa, T., Shimo, Y., Oyama, G., Umemura, A., Ito, M., Hori, M., Aoki, S., Hattori, N., 2022. White matter microstructures in Parkinson's disease with and without impulse control behaviors. Ann. Clin. Transl. Neurol. 9, 253–263. https://doi.org/10.1002/acn3.51504.

Tanaka, K., Wada-Isoe, K., Nakashita, S., Yamamoto, M., Nakashima, K., 2013. Impulsive compulsive behaviors in Japanese Parkinson's disease patients and utility of the Japanese version of the Questionnaire for Impulsive-Compulsive Disorders in Parkinson's disease. J. Neurol. Sci. 331, 76–80. https://doi.org/10.1016/j.jns.2013.05.013.

Tessitore, A., Santangelo, G., De Micco, R., Giordano, A., Raimo, S., Amboni, M., Esposito, F., Barone, P., Tedeschi, G., Vitale, C., 2017. Resting-state brain networks in patients with Parkinson's disease and impulse control disorders. Cortex 94, 63–72. https://doi.org/10.1016/j.cortex.2017.06.008.

Tomlinson, C.L., Stowe, R., Patel, S., Rick, C., Gray, R., Clarke, C.E., 2010. Systematic review of levodopa dose equivalency reporting in Parkinson's disease. Mov. Disord. 25, 2649–2653. https://doi.org/10.1002/mds.23429.

Voon, V., Napier, T.C., Frank, M.J., Sgambato-Faure, V., Grace, A.A., Rodriguez-Oroz, M., Obeso, J., Bezard, E., Fernagut, P.O., 2017. Impulse control disorders and levodopa-induced dyskinesias in Parkinson's disease: an update. Lancet Neurol 16, 238–250. https://doi.org/10.1016/S1474-4422(17)30004-2.

Vriend, C., 2018. The neurobiology of impulse control disorders in Parkinson's disease: from neurotransmitters to neural networks. Cell Tissue Res. 373, 327–336. https://doi.org/10.1007/s00441-017-2771-0.

Wang, Y., Sun, Z., Zhou, Z., 2022. Aberrant changes of dynamic global synchronization in patients with Parkinson's disease. Acta Radiol. 2841851221094967 https://doi.org/10.1177/02841851221094967.

Weintraub, D., Claassen, D.O., 2017. Impulse control and related disorders in Parkinson's disease. Int. Rev. Neurobiol. 133, 679–717. https://doi.org/10.1016/bs.irn.2017.04.006.

Weintraub, D., David, A.S., Evans, A.H., Grant, J.E., Stacy, M., 2015. Clinical spectrum of impulse control disorders in Parkinson's disease. Mov Disord 30, 121–127. https://doi.org/10.1002/mds.26016.

Weintraub, D., Nirenberg, M.J., 2013. Impulse control and related disorders in Parkinson's disease. Neurodegener Dis 11, 63–71. https://doi.org/10.1159/000341996.

Weintraub, D., Siderowf, A.D., Potenza, M.N., Goveas, J., Morales, K.H., Duda, J.E., Moberg, P.J., Stern, M.B., 2006. Association of dopamine agonist use with impulse control disorders in Parkinson disease. Arch. Neurol. 63, 969–973. https://doi.org/10.1001/archneur.63.7.969.

Wichmann, T., Delong, M.R., 2006. Deep brain stimulation for neurologic and neuropsychiatric disorders. Neuron 52, 197–204. https://doi.org/10.1016/j.neuron.2006.09.022.

Yang, W., Liu, B., Huang, B., Huang, R., Wang, L., Zhang, Y., Zhang, X., Wu, K., 2016. Altered resting-state functional connectivity of the striatum in Parkinson's disease after levodopa administration. PLoS One 11, e0161935.

Zhang, G., Zhang, Z., Liu, L., Yang, J., Huang, J., Xiong, N., Wang, T., 2014. Impulsive and compulsive behaviors in Parkinson's disease. Front. Aging Neurosci. 6, 318. https://doi.org/10.3389/fnagi.2014.00318.